IEEE Access
Multidisciplinary | Rapid Review | Open Access Journal

Received March 15, 2018, accepted May 15, 2018, date of publication June 5, 2018, date of current version July 6, 2018.

Digital Object Identifier 10.1109/ACCESS.2018.2839064

Analysis and Performance Optimization of LoRa Networks With Time and Antenna Diversity

ARLIONES HOELLER, Jr.,[1,2], (Student Member, IEEE), RICHARD DEMO SOUZA,[2], (Senior Member, IEEE), ONEL L. ALCARAZ LÓPEZ,[3], (Student Member, IEEE), HIRLEY ALVES,[3], (Member, IEEE), MARIO DE NORONHA NETO[1], AND GLAUBER BRANTE[4], (Member, IEEE)

[1]Department of Telecommunications Engineering, Federal Institute of Education, Science and Technology of Santa Catarina, São José 88103-310, Brazil
[2]Department of Electrical and Electronics Engineering, Federal University of Santa Catarina, Florianópolis 88040-900, Brazil
[3]Centre for Wireless Communications, University of Oulu, 90014 Oulu, Finland
[4]Department of Electrical Engineering, Federal University of Technology–Paraná, Curitiba 81280-340, Brazil

Corresponding author: Arliones Hoeller, Jr., (arliones.hoeller@ifsc.edu.br)

This work was supported in part by CNPq, Brazil, and in part by the Academy of Finland 6Genesis Flagship under Grant 318927.

ABSTRACT Low power wide area network (LPWAN) technologies are increasingly catching the attention of the Internet-of-Things market and have brought the need for reliable knowledge about the performance of such networks. This paper is concerned with the performance and scalability of LoRa networks, a leading LPWAN technology. Several recently published articles have analyzed the ability of LoRa networks to scale, i.e., their ability to support increased traffic and number of nodes. This paper proposes to employ message replication and gateways with multiple receive antennas to achieve, respectively, time and spatial diversity. The paper presents the proposed schemes and evaluates them through theoretical analysis and computer simulations. Results show that LoRa networks are highly sensitive to the increase in user and traffic density, but both message replication and multiple antennas can enhance performance. Message replication has an optimum number of message copies for each network configuration, and its utilization is more beneficial in low-density networks, while the use of multiple receive antennas at the gateway is always beneficial.

INDEX TERMS Internet-of-Things, long-range low-power communications, LoRa, communication diversity.

I. INTRODUCTION

The recent years saw the proliferation of the Internet-of-Things (IoT) pushed by inexpensive, Internet-connected devices using off-the-shelf components. The growth in the number of connected devices, however, turned the spotlight towards the limits of current connectivity technologies like WiFi, Bluetooth, and ZigBee, in terms not only of cost and size but also network capacity, communication range, and energy consumption [1]. Within this context, the Low Power Wide Area Network (LPWAN) technologies emerged to serve the market of Massive IoT (mIoT) [2], i.e., non-critical, low-power and low-cost applications tolerant to small data-rates and high latency. Among the most prominent LPWAN technologies in the market, today, are LoRaWAN, SigFox, and RPMA [3].

Although LPWAN technologies are in fast-paced adoption, reports on deployments with large numbers of stations are yet to come out, making their performance and capacity models still an open problem. As a result, recent studies have explored the capacity limits of the technologies and proposed techniques to enhance their performance.

This paper focuses on the aspects of the uplink of the LoRa (Long-Range) technology - the underlying proprietary physical layer (PHY) layer of LoRaWAN networks [4]. The problem under investigation is that of increasing the coverage probability in LoRa networks using time and antenna diversity [5]. More specifically, this paper analyzes the impact that message replication and gateways with multiple receive antennas have on the outage probability. We accomplished that by extending the outage models previously published by Georgiou and Raza [6] to account for the proposed diversity techniques. Additionally, simulations are used to validate the theoretical modeling, and the analysis of the results yields the formulation of an optimization problem that finds the optimum number of message replications for a set of network configuration parameters and different network density (number of nodes and their duty cycles).

A. RELATED WORK

Several recent related works have sought to evaluate the performance of LoRa networks using analytic modeling [6]–[10] and real measurements [11]–[19]. Additionally, a few techniques have been proposed to enhance the performance of LPWANs in general, with potential modifications to the current technologies, as for LoRa in [20]–[23], UNB/SigFox in [24], and for others in [25] and [26].

Analytic models have been proposed for a variety of scenarios and communication phenomena. Bor *et al.* [7] experimentally observed the capture effect of LoRa and modeled the capacity of such networks, concluding that LoRa networks with only one gateway and conservative operational parameters do not scale well, while networks with dynamic adaptation of operating parameters or multiple gateways tend to scale better. Georgiou and Raza [6] propose an analytic model that takes into account Rayleigh fading and allows to equate the coverage probabilities of nodes in a network considering two outage probabilities: disconnection and collision. Their work shows that LoRa networks are sensitive to network density. Gupta *et al.* [8] modeled the IoT traffic considering periodic messages and event-generated messages and analyzed the impact of traffic variations in LoRaWAN networks. They were able to identify that LoRa gateways do not handle well burst events, which generate a significant amount of messages in a short period, especially when there is a spatial or temporal correlation in the transmission behavior of IoT devices. Pop *et al.* [9] evaluated how LoRaWAN downlink impacts LoRa uplink goodput and coverage probability. They considered the medium access control (MAC) layer and, through simulations, verified that if too many end-devices request delivery confirmation, the downlink becomes unstable and unable to deliver several acknowledgment packets, thus forcing network nodes to retry their transmissions, ultimately flooding the network. Bankov *et al.* [10] proposed a mathematical model for LoRaWAN channel access taking into account the capture effect and using the Okumura-Hata model, but without fading. Concerning the modeling of communication fading, only Georgiou and Raza [6] and Pop *et al.* [9] take this impairment into account, to the best of our knowledge.

Several works have used measurements to evaluate the performance of LoRa networks. Petäjäjärvi *et al.* [11], [12] analyze Doppler robustness, scalability, and coverage of LoRa networks and report the experimental validation of such metrics in terrestrial and water environments for static and mobile nodes. Considering a delivery ratio of at least 60% and LoRa most conservative configurations, they were able to communicate to static nodes ranging up to 30 km over the water and up to 10 km on the ground. Regarding Doppler robustness, they observed that communication degrades significantly when the velocity of the node in relation to the gateway is above 40 km/h. There are similar reports of LoRa measurements done in different environments, including a university campus [13], indoor applications [14], industry [15], dense cities downtown [16], [17], smart metering [18], and rural areas [19]. Albeit these measurements show interesting results, it is important to note that none of them used a large number of network nodes, thus making it difficult to validate models for dense networks.

A few recently published work also propose some enhancements to LoRa. Cuomo *et al.* [20] propose algorithms to replace LoRaWAN adaptive data rate strategy. The proposed algorithms do not base the configuration of the spreading factor (SF) on distance and received power measurements, but take into account the number of connected devices, allowing the equalization of the time-on-air (ToA) of the packets in each SF. Bor and Roedig [21] explore LoRa configuration parameters such as SF, bandwidth, coding rate and transmission power, which result in 6, 720 possible settings, and proposes an optimization problem that minimizes energy spent on data transmission while meeting required communication performance. Qin and McCann [22] approach the optimization of LPWANs efficiency from a resource allocation perspective. They use game theory to derive an algorithm that allows network nodes to decide which channel and SF to use and, for each channel/SF group, which is the optimal transmit power that maximizes data extraction rate. Voigt *et al.* [23] consider the inter-network interference that is likely to take place when several independent LoRa networks get deployed too close. Authors consider using directional antennas in network nodes and using multiple gateways in the network. Results show that directional antennas enhance data extraction rate, although the use of multiple gateways in the covered area tends to perform better.

Besides the above works, some authors have explored techniques similar to those proposed in this paper for LoRa, UNB/SigFox, or for LPWANs in general. Mo *et al.* [24] investigated the optimal number of message replications for use in UNB/SigFox networks. Song *et al.* [25] consider the macro reception diversity of long-range ALOHA networks, where augmented spatial diversity arises from allowing several base stations to receive the same packet. Magrin *et al.* [26] developed a simulation model for the NS-3 network simulator with which they showed that LoRa networks support a large number of nodes and maintain reasonable network quality if several gateways are carefully placed.

In this paper, we model and validate the behavior of LoRa networks using message replication to exploit time diversity and using a single gateway with multiple receive antennas to exploit spatial diversity, striving to maximize network performance. To do that, we take the work of [6] as baseline model and extend it to incorporate the proposed techniques. Our work on message replication differs from [24] because that work considers UNB networks where each transmission uses a random central frequency – an assumption that changes the collision model. Moreover, our work takes fading into account, what [24] does not. Our approach using multiple receive antennas differs from [25] and [26] because they consider spatial diversity generated by multiple gateways. Our work examines the case where multiple receive antennas in a single gateway create signal diversity able to enhance

signal quality, an approach that can be naturally extended to the case of multiple gateways in the future. To the best of our knowledge, no work has investigated the use of multiple receive antennas and message replications in LoRa networks.

B. CONTRIBUTIONS

The contributions of this work can be summarized as:

- The optimization of the number of message copies for each SF configuration that maximizes network coverage probability in LoRa networks;
- The formulation of a tight closed-form bound for the collision probability considering gateways with multiple receive antennas;
- The analysis of the interaction between message replication and multiple receive antennas in LoRa networks, showing that message replication brings benefits only for low-density networks, while multiple receive antennas are always beneficial.

C. ORGANIZATION

The remaining of this paper is organized as follows. Section II introduces the LoRa technology. Section III briefly presents Georgiou and Raza model [6], which is the basis upon which we build the contributions of this paper. Section IV introduces and analyzes the model extensions to support message replications and time diversity. Section V introduces and analyzes the extensions to support multiple receive antennas in a gateway and exploit spatial diversity. Section VI shows and discusses the results of numerical simulations. Section VII makes final remarks and proposes future work.

Finally, Table 1 provides a list of symbols used in this paper.

TABLE 1. List of symbols.

$\mathbb{S}$	Spreading Factor
B	Bandwidth
N	Number of nodes
$\bar{N}$	Average number of nodes
R	Radius of the covered area
V	Covered area
Φ	PPP of nodes distribution
ρ	PPP density
d_i	Euclidean distance of the i-th node from the gateway
$\mathcal{P}_i$	Transmit power of the i-th node
$g(d_i)$	Path loss attenuation for transmission distance d_i
h_i	Rayleigh fading affecting a transmission from node i
λ	RF wavelength
η	Path loss exponent
r_i	Signal of the i-th node received at the gateway
s_i	Signal transmitted by the i-th node
$\chi_k^{\mathbb{S}}$	Function indicating if node k is transmitting using S
n	Additive White Gaussian Noise (AWGN)
$\mathcal{N}$	Variance of the AWGN
F	Noise Figure
$q_{\mathbb{S}}$	SNR threshold for successful reception of the signal
H_1, Q_1	Connection and capture probabilities
$H_{1,M}, Q_{1,M}$	Connection and capture probabilities using M message replicas
$H_{1,A}, Q_{1,A}$	Connection and capture probabilities using A receive antennas
$\wp_c$	Average coverage probability
$\wp_{c,i}$	Average coverage probability inside the i-th annulus
l_i, l_{i+1}	Respectively, inner and outer radii of the i-th annulus
M	Number of message replicas
A	Number of receive antennas in the gateway
S_i	Set of reception events
$i,\ j,\ k,\ t,\ z$	Used as indexes in iterative functions

II. LPWANs AND LoRa

LPWANs employ low-power communication technologies that enable the connection of thousands of IoT devices across long distances. Most of these technologies work in frequencies below 1 GHz and employ modulation techniques that enable link budgets of 150 ± 10 dB, resulting in robust communication channels with low energy consumption reaching distances in the order of kilometers [27], [28]. Additionally, for reducing complexity and energy consumption, LPWAN technologies use MAC protocols, which may decrease the efficiency of channel use. For instance, both LoRaWAN and SigFox transmit data using unslotted ALOHA, therefore without previously checking if the channel is in use. ALOHA networks are known to present high collision probability when a large number of stations are connected [29].

A. LoRa

LoRa is a proprietary sub-GHz chirp spread spectrum modulation technique optimized for long-range applications and low power consumption at a low transmission rate [4], which enables the LPWAN paradigm. The technology allows the use of variable transmission rates with constant bandwidth using different orthogonal SFs. The variable data rate characteristic allows optimizing applications according to range, robustness or energy consumption. With the use of different SFs, it is also possible that several devices perform data transmission at the same time, using the same channel frequency without relevant degradation of the received signal.

LoRa modulation depends, basically, on three parameters [30]: bandwidth (B), usually set to 125 kHz or 250 kHz for uplink and 500 kHz for downlink; SF, denoted in the equations by $\mathbb{S} \in \{7, \cdots, 12\}$; and the forward error correction rate (FEC), varying from $\frac{4}{8}$ to $\frac{4}{5}$. It is possible to extract from these parameters the packet Time-on-Air (ToA), the receiver sensitivity and the required signal to noise ratio (SNR) for successful detection in the absence of interference. Table 2 shows the relation among LoRa parameters for a payload of 9 bytes at $B = 125$ kHz with CRC and Header Mode enabled. It is possible to observe that ToA grows exponentially with SF, reducing the bit rate while increasing the receiver sensitivity, thus allowing higher coverage.

TABLE 2. LoRa Uplink Characteristics considering packets of 9 bytes at $B = 125$ kHz with CRC and Header Mode enabled.

SF	Time-on-Air (ms)	R_b (kbps)	Receiver Sensitivity (dBm)	SNR threshold $q_{\mathbb{S}}$ (dB)
7	41.22	5.47	-123	-6
8	72.19	3.12	-126	-9
9	144.38	1.76	-129	-12
10	247.81	0.98	-132	-15
11	495.62	0.54	-134.5	-17.5
12	991.23	0.29	-137	-20

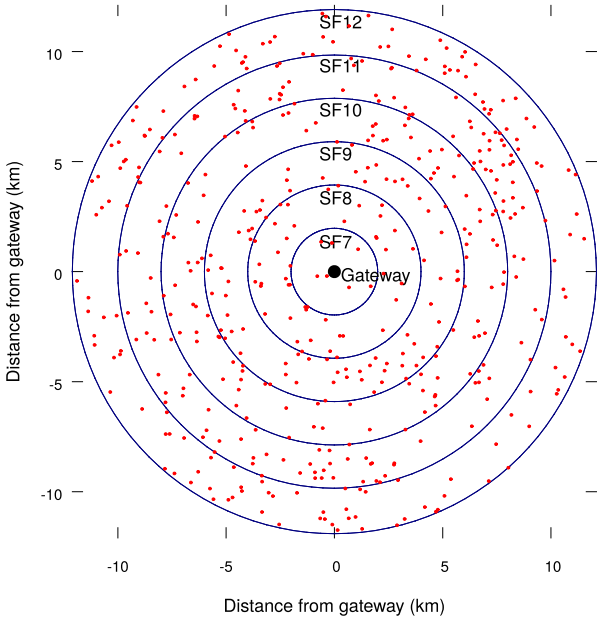

FIGURE 1. $\bar{N} = 500$ nodes uniformly distributed in a circular area of radius $R = 12000$ m around the gateway and with increasing SF every 2000 m.

The implementation of LoRa physical layer is agnostic of higher layers. One of the most widely used protocol stacks featuring a LoRa PHY is LoRaWAN, which implements a star topology and defines three types of devices: the *end-devices* (nodes), connected through a single-hop to one or more *gateways*, which in turn connect to a *network server* via an IP network. LoRaWAN MAC is performed using unslotted ALOHA [29].

Moreover, the hardware of a LoRa gateway can process up to nine channels in parallel, combining different sub-bands[1] and SFs [1]. Besides that, LoRa features the capture effect, making it possible to recover a LoRa signal when two or more signals are received simultaneously, using the same frequency and the same SF, provided that the desired signal be at least 6 dB stronger than any other [7].

III. SYSTEM MODEL

Following [6], consider that, on average, $\bar{N}$ nodes are uniformly distributed around a gateway in a circular region of radius R and area $V = \pi R^2$. In the coordinate system presented in Figure 1, the gateway is at the origin, and the nodes are deployed uniformly at random in the region $V \subseteq \mathbb{R}^2$ and transmit at random times. This distribution is described by an inhomogeneous Poisson point process (PPP) Φ with density $\rho > 0$ in V and 0 otherwise. In this scenario, d_i is the Euclidean distance between the gateway and the i-th node. Devices transmit in the uplink at random using the ALOHA protocol, obeying a duty cycle p_0. Finally, SF is assigned according to the distance from the gateway d_i, increasing every 2000 m, while all nodes transmit with the same power $\mathcal{P}_i$.

The uplink model considers that both path loss attenuation $g(d_i)$ and Rayleigh fading h_i affect the received signal, as in [6]. Path loss follows the Friis transmission equation $g(d_i) = \left(\frac{\lambda}{4\pi d_i}\right)^{\eta}$, where λ is the wavelength, and $\eta \geq 2$ is the path loss exponent. Rayleigh fading is modeled as a zero-mean, independent, circularly-symmetric complex Gaussian random variable with unit variance. Given a signal transmitted by a LoRa node s_1, the received signal at the gateway, r_1, is the sum of the attenuated transmitted signal, interference and noise. It can be expressed as

$$r_1 = g(d_1)h_1\, s_1 + \sum_{k=2}^{N} \chi_k^{\mathbb{S}} g(d_k) h_k s_k + n, \tag{1}$$

where $\chi_k^{\mathbb{S}}$ is an indicator function equal to 1 if the k-th node is transmitting in the same SF of the desired signal at a given time or 0 otherwise, and n is additive white Gaussian noise (AWGN) with zero mean and variance $\mathcal{N} = -174 + F + 10\log(B)$ dBm, where F is the receiver noise figure, and B is the channel bandwidth.

The outage probability model follows [6], where the authors consider that the outage of LoRa uplink occurs if either there is no connection between a node and the gateway or if there is a collision. This section briefly presents the probability models introduced in [6], which are the basis for the extensions that include time and antenna diversity presented in the next sections.

A. OUTAGE CONDITION 1: DISCONNECTION

First, we consider the connection probability, which depends on the communication distance. A node is assumed as *not* connected to the gateway if the SNR of the received signal is below the reception threshold that allows successful detection in the absence of interference. Different SFs result in different receiver sensitivities which, in turn, result in different SNR reception thresholds ($q_{\mathbb{S}}$), as shown in Table 2. The *connection probability* is thus

$$H_1 = \mathbb{P}[\text{SNR} \geq q_{\mathbb{S}} | d_1], \tag{2}$$

where $q_{\mathbb{S}}$ is the SNR reception threshold of the SF ($\mathbb{S}$) in use, and d_1 is the distance between the desired node and the gateway.

Since we assume Rayleigh fading, the instantaneous SNR is exponentially distributed [5], and therefore

$$H_1 = \mathbb{P}\left[|h_1|^2 \geq \frac{\mathcal{N} q_{\mathbb{S}}}{\mathcal{P}_1\, g(d_1)}\right] = \exp\left(-\frac{\mathcal{N} q_{\mathbb{S}}}{\mathcal{P}_1 g(d_1)}\right). \tag{3}$$

B. OUTAGE CONDITION 2: COLLISION

Since LoRa is a form of frequency modulation, it exhibits the capture effect [7], allowing stronger signals to suppress simultaneously received weaker signals. In LoRa, a collision only takes place if the power difference between the desired

[1] A LoRa sub-band is a set of frequency channels that devices in a network are configured to use.

signal and any other simultaneously received signal using the same SF and frequency channel is less than 6 dB. To evaluate this condition, one must consider the strongest interfering node k^* defined as

$$k^* = \underset{k>1}{\text{argmax}} \{\mathcal{P}_k \chi_k^{\mathbb{S}} |h_k|^2 g(d_k)\}. \quad (4)$$

Once k^* is found, the probability that no collision occurs or that the strongest interfering signal is at least 6 dB below the desired one, termed here as *capture probability*, is

$$\begin{aligned} Q_1 &= \mathbb{P}\left[\frac{|h_1|^2 \, g(d_1)}{|h_{k^*}|^2 \, g(d_{k^*})} \geq 4 \middle| d_1 \right] \\ &= \mathbb{E}_{|h_1|^2}\left[\mathbb{P}\left[X_{k^*} < \frac{|h_1|^2 g(d_1)}{4} \middle| |h_1|^2, d_1 \right] \right]. \end{aligned} \quad (5)$$

The above probability depends on the probability distribution of $X_{k^*} = |h_{k^*}|^2 \, g(d_{k^*})$. The cumulative distribution function (CDF) of X_{k^*} is derived in [6], and is denoted as $F_{X_{k^*}}$. Thus

$$\begin{aligned} Q_1 &= \mathbb{E}_{|h_1|^2}\left[F_{X_{k^*}}\left(\frac{|h_1|^2 g(d_1)}{4} \right) \right] \\ &= \int_0^\infty e^{-z} F_{X_{k^*}}\left(\frac{z g(d_1)}{4} \right) \mathrm{d}z. \end{aligned} \quad (6)$$

Moreover, Georgiou and Raza [6] present an approximation for (6) that is only accurate at the edges of each annulus in Figure 1. This paper considers only the exact probability in (6).

C. COVERAGE PROBABILITY

The *coverage probability* is the probability that the selected node is in coverage, *i.e.*, it can successfully communicate considering both the connection and collision outage conditions above. The coverage probability of the desired node is thus merely the product $H_1 Q_1$.

Moreover, the average coverage probability $\wp_c$ can be obtained by de-conditioning on the position of the desired node achieved by averaging in the network area,

$$\wp_c = \frac{2}{R^2} \int_0^R H_1(d_1) Q_1(d_1) d_1 \, \mathrm{d}d_1. \quad (7)$$

The remaining of this paper builds on the above model initially presented in [6] by including the required changes to take into account the effects of time and antenna diversity.

Additionally, different than [6], in this paper, we also consider the average coverage probability per SF (or per annulus). The coverage probability of a node in the annulus i is

$$\wp_{c,i} = \frac{2}{(l_{i+1} - l_i)^2} \int_{l_i}^{l_{i+1}} H_1(d_1) Q_1(d_1)(d_1 - l_i) \, \mathrm{d}d_1, \quad (8)$$

where l_i and l_{i+1} are, respectively, the inner and outer radii of the i-th annulus, as illustrated in Figure 1.

IV. MESSAGE REPLICATIONS - TIME DIVERSITY

Many systems increase network reliability by using some form of automatic repeat request (ARQ) techniques, in which receivers automatically request the retransmission of lost packets. Although LoRa systems can use such techniques, a recent study [9] has shown that LoRa downlink cannot support the high demand of acknowledgment packets generated when all nodes in a dense network request such confirmations, making delivery confirmation an unreliable feature. To increase network reliability, however, other techniques can be applied, being message replication one of them.

The first contribution of this paper is to analyze the effects of message replication in LoRa networks, where each information message is transmitted M times within the same time interval when message replication is not used. Therefore, with message replication, there is an M-fold increase in the network duty cycle. Such technique increases the temporal diversity of the desired signal, thus making it much more likely that at least one message copy arrives at the gateway. The increase in the connectivity success probability is dependent on the number of replications M.

First, consider the extension of the connection probability to the case of message replications, denoted by $H_{1,M}$. In this case, a connection outage only occurs if all M message copies are lost, therefore

$$H_{1,M} = 1 - (1 - H_1)^M, \quad (9)$$

where $|h_1|^2$ is assumed independent among replications. In a real deployment, one must consider that fading independence only takes place if the separation in time of each message copy is greater than the channel coherence time. In our simulations, we assume that this condition is always met [5].

Similar changes need to be made to the analysis of the capture probability. In this case, (5) can be rewritten to take into account the probability that at least one of the M message copies is received in the absence of interference or with the stronger interferer being at least 6 dB weaker,

$$Q_{1,M} = 1 - (1 - Q_1)^M. \quad (10)$$

It is important to highlight that the derivation of $F_{X_{k^*}}$ in [6], required for evaluating Q_1, defines the number of interfering nodes as a Poisson distribution with mean $\nu = p_0 \rho |\hat{V}(d_1)|$, where $\hat{V}(d_1)$ is the area of the annulus of the desired node. In the case of message replication, once the transmission of message copies increases the channel usage, when evaluating (10) it is necessary to proportionally increase the mean of the Poisson distribution by making $\nu = (M p_0) \rho |\hat{V}(d_1)|$.

We observed that the response of the average coverage probability ($\wp_{c,i}$) to variations in M shows an optimum point within the bounds of reasonable values of M. Thus, it is possible to define the following optimization problem in the form of an Integer Linear Program (ILP) to find the optimum integer number of message copies M^* for each SF in a given

network configuration. The ILP is

$$\begin{aligned} M^*(i) &= \arg\max_{M\in\mathbb{Z}} \wp_{c,i} \\ &= \arg\max_{M\in\mathbb{Z}} \left[\frac{2}{(l_{i+1}-l_i)^2} \int_{l_i}^{l_{i+1}} H_{1,M}(d1) Q_{1,M}(d1) \right. \\ &\quad \left. \times (d_1 - l_i) \mathrm{d}d_1 \right] \\ &\quad \text{subject to: } 1 \le M \le M_{\max}, \end{aligned} \tag{11}$$

where i is the annulus (and, thus, SF) under consideration and $M_{\max}$ is the maximum value considered for M^*. In this work, we solved this ILP by exhaustively enumerating $\wp_{c,i}$ for all possible values of M. This is a viable option since the set of possible values of M is small.

V. MULTIPLE RECEIVE ANTENNAS - SPATIAL DIVERSITY

The second contribution of this paper is to analyze the gain in coverage probability of LoRa networks when using multiple receive antennas at the gateway to achieving spatial diversity. Note that the application of a technique such as maximum ratio combining [5] is not feasible in this case, as we consider the use of commercial LoRa radios. As the gateway can only tune to a particular user if the Signal-Interference Ratio (SIR) is at least 6dB (considering nodes with the same SF), it would be not possible to combine several branches with SIRs below 6dB to achieve a combined signal with SIR of at least 6dB. The alternative, thus, is to consider an approach based on the selection combining technique [5].

In this case, the adaptation of the connection probability from (2) is straightforward. It is assumed that A receive antennas are sufficiently spaced apart so that the fading is independent among them. Therefore, successful connection in the absence of interference is achieved if the SNR in at least one of the antennas is above the detection threshold

$$H_{1,A} = 1 - (1 - H_1)^A. \tag{12}$$

By its turn, the capture probability is concerned with collisions from interfering signals and demands a more intricate mathematical development. Here, the strongest interfering signal seen by the i-th antenna is denoted by k_i^* and defined as

$$k_i^* = \underset{k>1}{\operatorname{argmax}} \{\mathcal{P}_k \chi_k^{\mathbb{S}} |h_{i,k}|^2 g(d_k)\}, \tag{13}$$

where $h_{i,k}$ is the channel fading of the k-th node and the i-th antenna. Thus, the probability that there is no collision in at least one of the antennas is

$$Q_{1,A} = \mathbb{P}\left[\max_{i=1,\cdots,A} \mathrm{SIR}_i^* < 4 \middle| d_1 \right], \tag{14}$$

$$\mathrm{SIR}_i^* = \frac{|h_{i,1}|^2 g(d_1)}{|h_{i,k_i^*}|^2 g(d_{k_i^*})}, \tag{15}$$

where $h_{i,1}$ is the channel fading of the desired node with antenna i, and SIR is the signal to interference ratio.

Note that the distribution of $X_{k_i^*} = |h_{i,k_i^*}|^2 \; g(d_{k_i^*})$ is correlated among antennas, as $g(d_{k_i^*})$ is the same for all antennas. Thus, it seems intractable to make analytic progress from (14). However, a lower bound on the capture probability can be obtained as

$$Q_{1,A} \ge \mathbb{P}\left[\max_{i=1,\cdots,A} \mathrm{SIR}_i < 4 \middle| d_1 \right] = Q_{1,A}^{\mathrm{lo}}, \tag{16}$$

where

$$\mathrm{SIR}_i = \frac{|h_{i,1}|^2 \; g(d_1)}{\sum\limits_{k>1}^{\mathbb{S}} \chi_k^{\mathbb{S}} |h_{i,k}|^2 g(d_k)} = \frac{|h_{i,1}|^2 d_1^{-\eta}}{I_i}, \tag{17}$$

with

$$I_i = \sum_{k>1}^{\mathbb{S}} \chi_k^{\mathbb{S}} |h_{i,k}|^2 d_k^{-\eta}. \tag{18}$$

Compared with (14), in this case, we consider the sum of all interfering signals instead of the stronger interfering signal only. Since $\mathrm{SIR}_i < \mathrm{SIR}_i^*$, (16) is a lower bound. As we shall see in Section VI, the bound can be very tight if concurrent transmissions from more than two devices are not frequent, which is expected in most LoRa scenarios, since duty cycle is typically very low [8].

To evolve on the mathematical analysis, we consider the development presented by Haenggi [31]. Let us define the events $S_i \triangleq \{\mathrm{SIR}_i > 4\}$. We focus first on the probability of the joint occurrence of z of these events,

$$P_z \triangleq \mathbb{P}\left[\bigcap_{i=1,\cdots,z} S_i \right], \tag{19}$$

i.e., the probability that the SIR exceeds 6 dB at z antennas at the same time. Thus,

$$P_z = \mathbb{P}[|h_{1,1}|^2 > 4 d_1^{\eta} I_1, \cdots, |h_{z,1}|^2 > 4 d_1^{\eta} I_z]. \tag{20}$$

Since I_i, $i \in \{1, \cdots, z\}$, are correlated through the common randomness Φ (the point process of the nodes) and $|h_{i,1}|^2$ is exponentially distributed, we have that

$$\begin{aligned} P_z &= \mathbb{E}\left[e^{-4 \, d_1^{\eta} \, I_1}, \cdots, e^{-4 \, d_1^{\eta} \, I_z} \right] = \mathbb{E}\left[\prod_{i=1}^{z} e^{4 \, d_1^{\eta} \, I_i} \right] \\ &= \mathbb{E}\left[\prod_{i=1}^{z} \prod_{k\in\Phi} e^{-4 d_1^{\eta} \chi_k^{\mathbb{S}} |h_{i,k}|^2 \, d_k^{-\eta}} \right] \\ &= \mathbb{E}\left[\prod_{k\in\Phi} \left(\frac{1}{1 + 4 \, d_1^{\eta} \chi_k^{\mathbb{S}} d_k^{-\eta}} \right)^z \right] \\ &= \exp\left(-2\pi\rho p_0 \int_{l_j}^{l_{j+1}} d_k \left(1 - \left(\frac{1}{1 + 4 \, d_1^{\eta} \chi_k^{\mathbb{S}} d_k^{-\eta}} \right)^z \right) \mathrm{d}d_k \right) \\ &\overset{(a)}{=} \exp\left(-\frac{2\pi\rho p_0 \chi_k^{\mathbb{S}} d_k^2}{4 + 2z\eta} \left(2 + z\eta - 2 \left(\frac{\chi_k^{\mathbb{S}} d_k^{-\eta}}{4 d_1^{\eta}} \right)^z \right. \right. \\ &\quad \left. \left. {}_2F_1(z, z+\frac{2}{\eta}; 1+z+\frac{2}{\eta}; -\frac{\chi_k^{\mathbb{S}} d_k^{-\eta}}{4 d_1^{\eta}}) \right) \Big|_{d_k=l_j}^{d_k=l_{j+1}} \right), \end{aligned} \tag{21}$$

where step (a) uses the definition of the hypergeometric function [32].

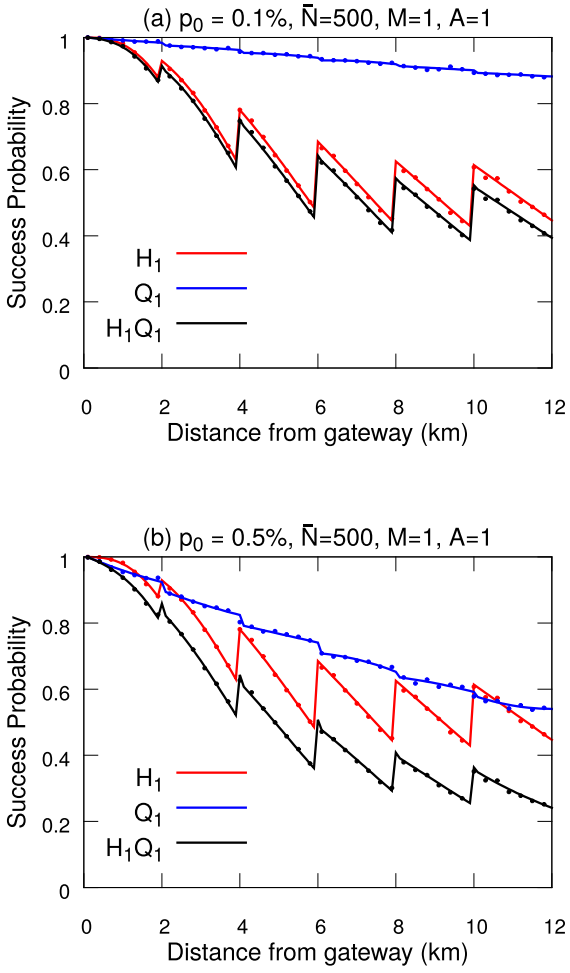

FIGURE 2. Performance of LoRa uplink baseline model ($M = 1$ and $A = 1$), with an average number of nodes $\bar{N} = 500$ and varying duty cycle p_0.

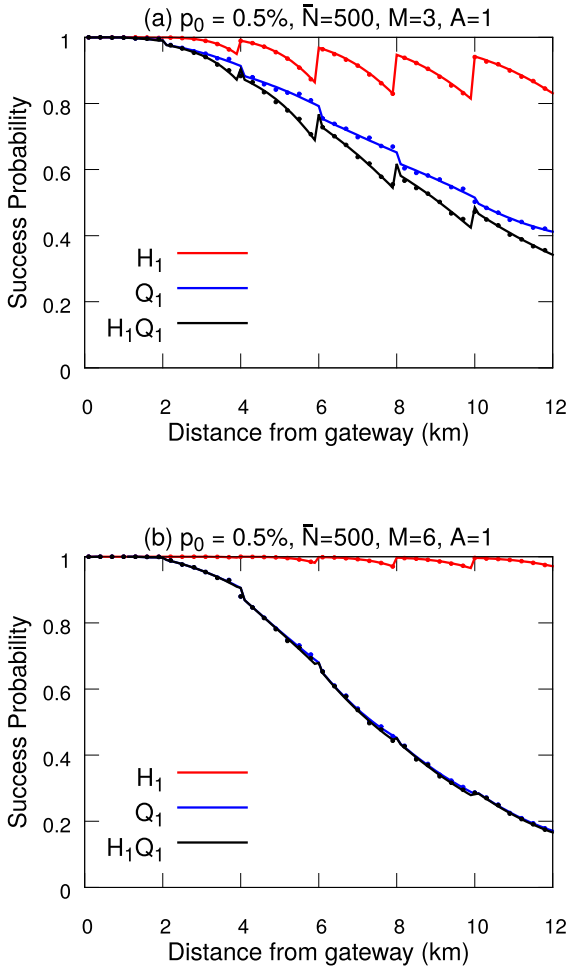

FIGURE 3. Impact of message replication in LoRa uplink, with an average number of nodes $\bar{N} = 500$, a duty cycle of $p_0 = 0.5\%$, a single antenna ($A = 1$), and a varying number of message copies M.

Finally, a transmission is successful if the SIR in at least one of the A antennas is higher than the threshold, thus:

$$Q_{1,A}^{lo} \triangleq \mathbb{P}\left(\bigcup_{i=1}^{A} S_i\right) = \sum_{i=1}^{A} (-1)^{i+1} \binom{A}{i} P_i. \qquad (22)$$

VI. NUMERICAL RESULTS

This section evaluates the proposed models using numerical simulations. In the figures shown here, solid lines represent theoretical probabilities while points of the same color represent the results of Monte Carlo simulations. Each simulation point is the averaged result of 10^5 random deployment scenarios. Results are shown for $p_0 = \{0.1, 0.5\}\%$, which is equivalent to $\{3.6, 18.1\}$ messages per hour with $\mathbb{S} = 12$, or $\{87.3, 436.7\}$ messages per hour with $\mathbb{S} = 7$. These are worst-case considerations of the LoRa reality. In practice, typical LoRa applications are expected to operate with duty cycles below 0.1%, and rarely above 0.5% [8]. Moreover, following [6], all results presented in this paper consider $F = 6$ dBm, $\eta = 2.75$, $\lambda = c/f$ m, $f = 868$ MHz, $B = 125$ kHz, which are typical configurations for sub-urban scenarios following European regulations.

A. BASELINE MODEL - WITHOUT DIVERSITY

Figure 2 shows the performance of the baseline model of Section III, with varying duty cycle and an average number of nodes of $\bar{N} = 500$, without any time or antenna diversity, *i.e.*, $M = 1$, $A = 1$. There is no need to vary both duty cycle and the average number of nodes in the simulations because the model is sensitive to the medium usage, the product $p_0\bar{N}$, rather than on these parameters separately. The figure shows the connection probability H_1, capture probability Q_1, and coverage probability H_1Q_1 in separated curves. As expected, results for H_1 are not dependent on duty cycle or the average number of nodes because H_1 models the connection probability, which depends only on the distance. It makes Q_1 primarily responsible for network quality degradation. That happens because Q_1 takes interference into account, which is substantially affected by increasing medium usage.

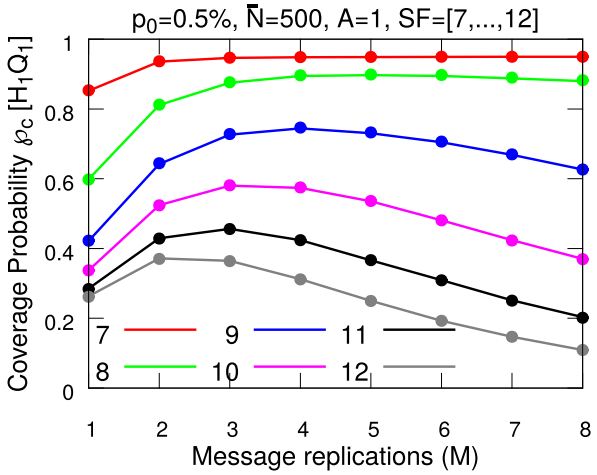

FIGURE 4. Coverage probabilities of LoRa network with average number of nodes $\bar{N} = 500$ and duty cycle $p_0 = 0.5\%$ for each SF ($\mathbb{S} \in \{7, \cdots, 12\}$).

It is also possible to note that Q_1 decreases with SF, what is expected behavior and happens due to the combination of two factors. The first one is that ToA increases with SF (see Table 2). The second one is that, because outer annuli are bigger than inner annuli, and nodes are distributed uniformly in the circular region around the gateway, the scenario has more nodes using higher SFs.

B. MESSAGE REPLICATION

Figure 3 shows the impact of the message replication approach for $M = \{3, 6\}$ message copies using the same network configuration of the results presented in Figure 2(b), except for the value of M. As expected, message replication has a substantial positive impact on $H_{1,M}$ because M decreases this outage condition exponentially. For $Q_{1,M}$, however, the positive impact only exists as long as the message copies do not flood the network, reaching a point where the number of collisions is too high. Moreover, message replication performs better in lower SF than higher SF, what happens because ToA nearly doubles for each SF increase, making it faster to flood the network with message replications when using higher SFs.

Figure 4 shows the average coverage probability $\wp_{c,i}$ with each value of SF, for a varying number of message copies M. It is possible to observe that the best number of message replications is different for each SF configuration. Table 3 summarizes, for each SF and the entire network, the optimum number of message copies (M^*) and the corresponding average coverage probability for the annulus that is using that SF. The last column of the table shows the average coverage probability of the network if each node uses the M^* computed for its SF. To allow comparison, the last line of the table shows the coverage probability without message replication. Note that the optimum number of message copies is a decreasing function of the SF, what makes sense since message replications increase the network density.

TABLE 3. Optimum values of M and the respective average coverage probability $\wp_c$ for each SF and the whole network ($p_0 = 0.5\%$ and $\bar{N} = 500$).

$\mathbb{S}$	7	8	9	10	11	12	Network
M^*	8 94.9%	5 89.7%	4 74.4%	3 58.0%	3 45.6%	2 37.2%	2, 3, 4, 5, 8 59.7%
$M = 1$	85.2%	59.9%	42.2%	33.7%	28.5%	26.3%	39.4%

TABLE 4. Optimum M* for different configurations of network density and number of Antennas.

		$\bar{N} = 500$		$\bar{N} = 1000$		$\bar{N} = 1500$	
p_0	A	M^*	$\rho_c[H_1Q_1]$	M^*	$\rho_c[H_1Q_1]$	M^*	$\rho_c[H_1Q_1]$
0.1%	**1**	8	99.7%	5	91.0%	4	79.1%
	2	4	100.0%	5	96.6%	4	89.2%
	4	3	100.0%	5	99.5%	3	95.8%
	8	2	100.0%	3	100.0%	4	99.4%
0.5%	**1**	3	59.2%	2	33.0%	2	20.5%
	2	3	73.3%	2	47.1%	1	33.3%
	4	2	85.6%	1	61.6%	1	49.1%
	8	2	94.0%	1	76.5%	1	64.2%

C. MULTIPLE RECEIVE ANTENNAS

Figure 5 shows the performance for $A = \{1, 2, 4\}$ receive antennas at the gateway, in a scenario with $p_0 = 0.5\%$, $\bar{N} = 500$ and $M = 1$. It is evident the tightness of the lower bound given in (22). In a different way from what happens with message replication, the growth of the delivery probability in LoRa networks with multiple receive antennas is a monotonic function of the number of antennas A. The more receive antennas a gateway has, the better. Figures 5(b) and 5(c) show that multiple receive antennas bring an average gain in H_1Q_1 probability of 1.5× and 1.97× for, respectively, $A = 2$ and $A = 4$. This gain results in the average coverage $\wp_c[H_1Q_1]$ going from 39.44% to 59.27% and 77.69%, respectively.

Table 4 presents the performance for the integration of both time and antenna diversity. It shows the average coverage probability $\wp_c[H_1Q_1]$ in the deployment area for different duty cycles (p_0), different average number of nodes ($\bar{N}$), and a varying number of receive antennas (A). Results consider the optimum number of message copies (M^*) for each configuration. It is possible to conclude that low-density networks like the ones with $p_0 = 0.1\%$, $\bar{N} = 500$ can achieve performance gains with message replication alone. Networks slightly more dense like the ones with $p_0 = 0.1\%$, $\bar{N} = \{1000, 1500\}$ can achieve reasonably high performance gains by combining both techniques. Performance gains for dense networks, on the other hand, depend much more on antenna diversity to achieve larger benefits, since message replications contribute to an excessive increase in collision probability. The denser cases shown in Table 4, $p_0 = 0.5\%$, $\bar{N} = \{1000, 1500\}$, demonstrate that message replication may not be an option for similar cases. Regardless of the network density, the results show that the careful use of both techniques can achieve significant gains.

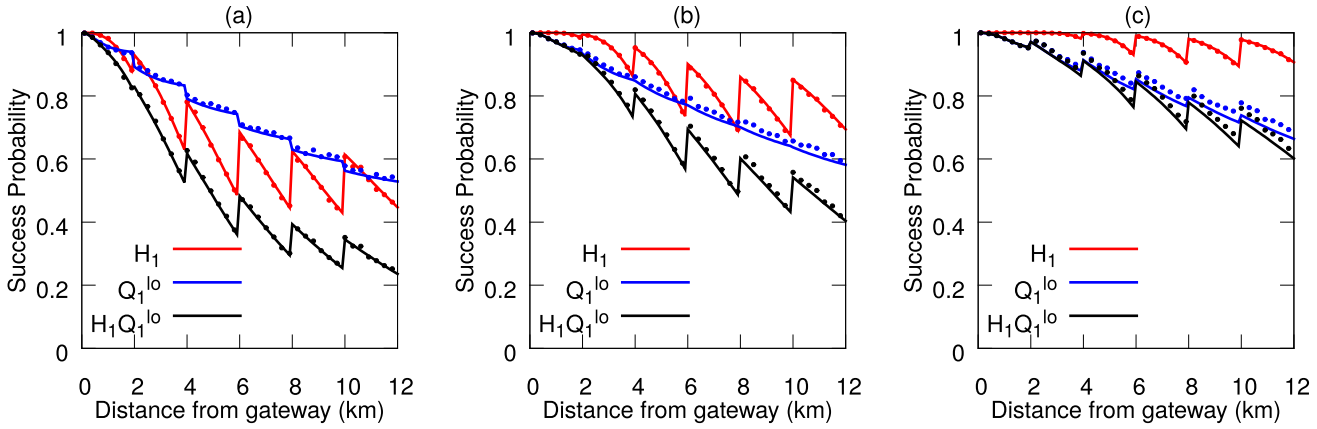

FIGURE 5. Impact of multiple receive antennas at the LoRa gateway, considering an average number of nodes $\bar{N} = 500$, a duty cycle of $p_0 = 0.5\%$, a single message copy ($M = 1$), and different numbers of receive antennas A.

VII. CONCLUSIONS AND FUTURE WORK

This paper analyzed the use of time and spatial diversity to enhance the uplink performance in LoRa networks through message replication and multiple receive antennas. Theoretical modeling and computer simulations were used to investigate the proposed methods. For message replication, there is an optimal number of copies to be employed in each network configuration. Moreover, replication is very useful in low-density networks, while multiple receive antennas are always beneficial. Finally, the adequate combination of both techniques can considerably improve the network performance.

Future work can consider the optimization of message replication taking into account energy efficiency, as well as the allocation of different M for different users in a way to favor nodes that require a larger Quality-of-Service (QoS). Moreover, spatial diversity can also be exploited in a macro sense, with multiple gateways with multiple receive antennas. The adequate allocation of SF for each user is also an interesting open problem in each of the above cases.

REFERENCES

[1] M. Centenaro, L. Vangelista, A. Zanella, and M. Zorzi, "Long-range communications in unlicensed bands: The rising stars in the IoT and smart city scenarios," *IEEE Wireless Commun.*, vol. 23, no. 5, pp. 60–67, Oct. 2016.

[2] "White paper: Cellular networks for massive IoT—Enabling low power wide area applications," Ericsson AB, Stockholm, Sweden, Tech. Rep. UEN 284 23-3278, Jan. 2016. [Online]. Available: https://www.ericsson.com/assets/local/publications/white-papers/wp_iot.pdf

[3] S. Andreev *et al.*, "Understanding the IoT connectivity landscape: A contemporary M2M radio technology roadmap," *IEEE Commun. Mag.*, vol. 53, no. 9, pp. 32–40, Sep. 2015.

[4] (Mar. 2018). *LoRa Alliance*. [Online]. Available: http://www.lora-alliance.org

[5] A. Goldsmith, *Wireless Communications*. New York, NY, USA: Cambridge Univ. Press, 2005.

[6] O. Georgiou and U. Raza, "Low power wide area network analysis: Can LoRa scale?" *IEEE Wireless Commun. Lett.*, vol. 6, no. 2, pp. 162–165, Apr. 2017.

[7] M. C. Bor, U. Roedig, T. Voigt, and J. M. Alonso, "Do LoRa low-power wide-area networks scale?" in *Proc. 19th ACM Int. Conf. Modeling, Anal., Simulation Wireless Mobile Syst. (MSWiM)*, New York, NY, USA, 2016, pp. 59–67.

[8] V. Gupta, S. K. Devar, N. H. Kumar, and K. P. Bagadi, "Modelling of IoT traffic and its impact on LoRaWAN," in *Proc. IEEE Global Commun. Conf. (GLOBECOM)*, Dec. 2017, pp. 1–6.

[9] A.-I. Pop, U. Raza, P. Kulkarni, and M. Sooriyabandara, "Does bidirectional traffic do more harm than good in LoRaWAN based LPWA networks?" in *Proc. IEEE Global Commun. Conf. (GLOBECOM)*, Dec. 2017, pp. 1–6. [Online]. Available: https://ieeexplore.ieee.org/document/8254509/

[10] D. Bankov, E. Khorov, and A. Lyakhov, "Mathematical model of LoRaWAN channel access with capture effect," in *Proc. IEEE 28th Annu. Int. Symp. Pers., Indoor, Mobile Radio Commun. (PIMRC)*, Oct. 2017, pp. 1–5.

[11] J. Petäjäjärvi, K. Mikhaylov, M. Pettissalo, J. Janhunen, and J. Iinatti, "Performance of a low-power wide-area network based on LoRa technology: Doppler robustness, scalability, and coverage," *Int. J. Distrib. Sensor Netw.*, vol. 13, no. 3, pp. 1–16, 2017.

[12] J. Petäjäjärvi, K. Mikhaylov, M. Hämäläinen, and J. Iinatti, "Evaluation of LoRa LPWAN technology for remote health and wellbeing monitoring," in *Proc. 10th Int. Symp. Med. Inf. Commun. Technol. (ISMICT)*, Mar. 2016, pp. 1–5.

[13] S.-Y. Wang *et al.*, "Performance of LoRa-based IoT applications on campus," in *Proc. IEEE 86th Veh. Technol. Conf. (VTC-Fall)*, Sep. 2017, pp. 1–6.

[14] P. Neumann, J. Montavont, and T. Noël, "Indoor deployment of low-power wide area networks (LPWAN): A LoRaWAN case study," in *Proc. Int. Conf. Wireless Mobile Comput., Netw. Commun. (WiMOB)*, 2016, pp. 1–8.

[15] L. Angrisani, P. Arpaia, F. Bonavolontà, M. Conti, and A. Liccardo, "LoRa protocol performance assessment in critical noise conditions," in *Proc. IEEE 3rd Int. Forum Res. Technol. Soc. Ind. (RTSI)*, Sep. 2017, pp. 1–5.

[16] P. Jörke, S. Böcker, F. Liedmann, and C. Wietfeld, "Urban channel models for smart city IoT-networks based on empirical measurements of LoRa-links at 433 and 868 MHz," in *Proc. IEEE 28th Annu. Int. Symp. Pers., Indoor, Mobile Radio Commun. (PIMRC)*, Oct. 2017, pp. 1–6.

[17] P. J. Radcliffe, K. G. Chavez, P. Beckett, J. Spangaro, and C. Jakob, "Usability of LoRaWAN technology in a central business district," in *Proc. IEEE 85th Veh. Technol. Conf. (VTC-Spring)*, Jun. 2017, pp. 1–6.

[18] M. Rizzi, P. Ferrari, A. Flammini, and E. Sisinni, "Evaluation of the IoT LoRaWAN solution for distributed measurement applications," *IEEE Trans. Instrum. Meas.*, vol. 66, no. 12, pp. 3340–3349, Dec. 2017.

[19] R. Oliveira, L. Guardalben, and S. Sargento, "Long range communications in urban and rural environments," in *Proc. IEEE Symp. Comput. Commun.*, Jul. 2017, pp. 810–817.

[20] F. Cuomo, M. Campo, G. Bianchi, G. Rossini, P. Pisani, and A. Caponi, "EXPLoRa: Extending the performance of LoRa by suitable spreading factor allocations," in *Proc. IEEE 13th Int. Conf. Wireless Mobile Comput., Netw. Commun. (WiMOB)*, Oct. 2017, pp. 1–8.

[21] M. Bor and U. Roedig, "LoRa transmission parameter selection," in *Proc. 13th Int. Conf. Distrib. Comput. Sensor Syst. (DCOSS)*, 2017, pp. 27–34.

[22] Z. Qin and J. A. Mccann, "Resource efficiency in low-power wide-area networks for IoT applications," in *Proc. IEEE Global Commun. Conf. (GLOBECOM)*, Dec. 2017, pp. 1–7.

[23] T. Voigt, M. Bor, U. Roedig, and J. M. Alonso, "Mitigating inter-network interference in LoRa networks," in *Proc. Int. Conf. Embedded Wireless Syst. Netw.*, Uppsala, Sweden: Junction Publishing, 2017, pp. 323–328.

[24] Y. Mo, M.-T. Do, C. Goursaud, and J.-M. Gorce, "Optimization of the predefined number of replications in a ultra narrow band based IoT network," in *Proc. Wireless Days (WD)*, Mar. 2016, pp. 1–6.
[25] Q. Song, X. Lagrange, and L. Nuaymi, "Evaluation of macro diversity gain in long range ALOHA networks," *IEEE Commun. Lett.*, vol. 21, no. 11, pp. 2472–2475, Nov. 2017.
[26] D. Magrin, M. Centenaro, and L. Vangelista, "Performance evaluation of LoRa networks in a smart city scenario," in *Proc. IEEE Int. Conf. Commun.*, May 2017, pp. 1–7.
[27] U. Raza, P. Kulkarni, and M. Sooriyabandara, "Low power wide area networks: An overview," *IEEE Commun. Surv. Tuts.*, vol. 19, no. 2, pp. 855–873, 2nd Quart., 2017.
[28] C. Goursaud and J. M. Gorce, "Dedicated networks for IoT: PHY/MAC state of the art and challenges," *EAI Endorsed Trans. Internet Things*, vol. 15, no. 1, pp. 1–11, Oct. 2015.
[29] N. Abramson, "THE ALOHA SYSTEM—Another alternative for computer communications," in *Proc. Fall Joint Comput. Conf.*, Dec. 1970, pp. 281–285.
[30] *AN120.22 LoRa Modulation Basics*, Semtech Coorporation, Camarillo, CA, USA, Mar. 2015.
[31] M. Haenggi, "Diversity loss due to interference correlation," *IEEE Commun. Lett.*, vol. 16, no. 10, pp. 1600–1603, Oct. 2012.
[32] A. B. O. Daalhuis, "Hypergeometric function," in *NIST Handbook of Mathematical Functions Paperback and CD-ROM*, F. W. J. Olver, D. W. Lozier, R. F. Boisvert, and C. W. Clark, Eds., 1st ed. New York, NY, USA: Cambridge Univ. Press, 2010, ch. 15, pp. 383–402.

ARLIONES HOELLER, Jr., (S'06) was born in Blumenau, Brazil. He received the B.Sc. and M.Sc. degrees in computer science from the Federal University of Santa Catarina (UFSC), Brazil, in 2004 and 2007, respectively, where he is currently pursuing the D.Sc. degree in electrical engineering. From 2007 to 2010, he acted as a Software Engineer with Brazilian companies, working on telecommunications and embedded systems projects. From 2010 to 2013, he was a Researcher with the Software/Hardware Integration Lab, UFSC. Since 2013, he has been a Lecturer with the Federal Institute of Education, Science and Technology of Santa Catarina, São José, Brazil. His research interests are wireless communications and networks, low-power distributed embedded, and real-time systems.

RICHARD DEMO SOUZA (S'01–M'04–SM'12) was born in Florianópolis, Brazil. He received the B.Sc. and D.Sc. degrees in electrical engineering from the Federal University of Santa Catarina (UFSC), Brazil, in 1999 and 2003, respectively. In 2003, he was a Visiting Researcher with the Department of Electrical and Computer Engineering, University of Delaware, USA. From 2004 to 2016, he was with the Federal University of Technology–Paraná, Brazil. Since 2017, he has been with UFSC, where he is currently an Associate Professor. His research interests include wireless communications and signal processing. He is a Senior Member of the Brazilian Telecommunications Society. He was a co-recipient of the 2014 IEEE/IFIP Wireless Days Conference Best Paper Award, a Supervisor of the Best Ph.D. Thesis in electrical engineering in Brazil in 2014, and a co-recipient of the 2016 Research Award from the Cuban Academy of Sciences. He has served as an Associate Editor for the IEEE COMMUNICATIONS LETTERS, the *EURASIP Journal on Wireless Communications and Networking*, and the IEEE TRANSACTIONS ON VEHICULAR TECHNOLOGY.

ONEL L. ALCARAZ LÓPEZ was born in Sancti-Spíritus, Cuba, in 1989. He received the B.Sc. degree (Hons.) in electrical engineering from the Central University of Las Villas, Cuba, in 2013, and the M.Sc. degree in electrical engineering from the Federal University of Paraná, Brazil, in 2017. He is currently pursuing the Ph.D. degree with the University of Oulu, Oulu, Finland. From 2013 to 2015, he served as a Specialist in telematics with Cuban telecommunication company (ETECSA). He joined the Centre for Wireless Communications, University of Oulu. He received a grant from CAPES/CNPq for his M.Sc. degree. His research interests are on wireless communication, specifically in ultra-reliable, low-latency communication for future networks, energy harvesting setups, and efficient access techniques for massive machine-type communications.

HIRLEY ALVES received the B.Sc. and M.Sc. degrees in electrical engineering from the Federal University of Technology–Paraná (UTFPR), Brazil, in 2010 and 2011, respectively, and the dual D.Sc. degree from the University of Oulu, Oulu, Finland, and UTFPR in 2015. He is currently an Adjunct Professor of machine-type wireless communications with the Centre for Wireless Communications, University of Oulu. He is actively working on massive connectivity and ultra-reliable low-latency communication. His research interests are wireless and cooperative communication, wireless full-duplex communication, PHY-security, and ultra-reliable communication mechanisms for future machine-type wireless networks. He was a co-recipient of the 2017 IEEE International Symposium on Wireless Communications and Systems Best Paper Award and the 2016 Research Award from the Cuban Academy of Sciences. He has acted as an organizer, the chair, and serves as a TPC and a tutorial lecturer to several renowned international conferences.

MARIO DE NORONHA NETO was born in Jacarezinho, Brazil. He received the B.Sc., M.Sc., and D.Sc. degrees in electrical engineering from the Federal University of Santa Catarina, Brazil, in 2000, 2002, and 2006, respectively. Since 2005, he has been with the Federal Institute of Education, Science and Technology of Santa Catarina (IFSC), São José, Brazil, where he is currently a Lecturer. From 2009 to 2011, he acted as the Head of Innovation Department, IFSC. From 2012 to 2016, he acted as the Dean of Research, Graduate Studies and Innovation, IFSC. His research interests include wireless communication and low-power wide area networks.

GLAUBER BRANTE (S'10–M'14) was born in Arapongas, Brazil. He received the D.Sc. degree in electrical engineering from the Federal University of Technology–Paraná, Curitiba, Brazil, in 2013. In 2012, he was a Visiting Researcher with the Institute of Information and Communication Technologies, Electronics and Applied Mathematics, Catholic University of Louvain, Belgium. He is currently an Assistant Professor with the Federal University of Technology–Paraná. His research interests include cooperative communication, HARQ, energy efficiency, and physical-layer security. He received the Best Ph.D. Thesis Award in electrical engineering in Brazil in 2014, and he was a co-recipient of the 2016 Research Award from the Cuban Academy of Sciences. Since 2018, he has been serving as an Associate Editor for the IEEE COMMUNICATIONS LETTERS.